Available online at www.sciencedirect.com
ScienceDirect
Bioorganic & Medicinal Chemistry 14 (2006) 7205–7212
Bioorganic & Medicinal Chemistry

Ester derivatives of annulated tetrahydroazocines: A new class of selective acetylcholinesterase inhibitors

Andrea Carotti,[a] Modesto de Candia,[a] Marco Catto,[a] Tatiana N. Borisova,[b] Alexey V. Varlamov,[b] Estefanía Méndez-Álvarez,[c] Ramón Soto-Otero,[c] Leonid G. Voskressensky[b] and Cosimo Altomare[a,*]

[a]*Department of Pharmaceutical Chemistry, University of Bari, Via E. Orabona 4, I-70125 Bari, Italy*
[b]*Organic Chemistry Department of the Russian peoples friendship University, 6 Miklukho-Maklaya St., Moscow 117198, Russia*
[c]*Group of Neurochemistry, Department of Biochemistry and Molecular Biology, Faculty of Medicine, University of Santiago de Compostela, S. Francisco 1, E-15782 Santiago de Compostela, Spain*

Received 2 May 2006; revised 20 June 2006; accepted 23 June 2006
Available online 14 July 2006

Abstract—A series of ester derivatives of annulated tetrahydroazocines, namely 2,3,6,11-tetrahydro-1*H*-azocino[4,5-*b*]indoles (**5**–**10**), 2,3,6,7-tetrahydro-1*H*-azocino[5,4-*b*]indoles (**11**–**14**), and 4,7,8,9-tetrahydro-1*H*-pyrrolo[2,3-*d*]azocines (**15**–**18**), synthesized through an efficient 6 → 8 membered ring expansion procedure, were investigated for their acetylcholinesterase (AChE) inhibitory activities. Most of the compounds acted as AChE inhibitors in vitro, with IC_{50} values ranging from 5 to 40 μM. The most potent compounds **11** and **15**, both as racemic mixtures, proved selective toward AChE, exhibiting selectivity ratios versus butyrylcholinesterase (BuChE) of ca. 15 and more than 20, respectively. Structure–activity studies highlighted, among other factors, lipophilicity as a property modulating the AChE inhibition potency, as shown by a reasonable parabolic correlation between pIC_{50} and experimental 1-octanol/water partition coefficient (log *P*), which described the prevailing behavior of the examined compounds ($r^2 = 0.665$). Molecular docking simulations using the X-ray crystal structure of AChE from *Torpedo californica* suggested possible binding modes of the tetrahydroazocine ester derivatives **11** and **15**.

1. Introduction

Medium-sized N-heterocycles, in particular eight-membered azocines, are key structures occurring in many natural products.[1,2] Despite their bioactivity,[3] azocine fused ring systems are not sufficiently investigated, one barrier to their achievement generally being unsatisfactory synthetic procedures.[4]

The efficient construction of medium-sized cycles has attracted considerable attention during the past years, and recently some of us have reported a tandem Michael addition–nucleophilic substitution sequence involving dimethylacetylene dicarboxylate (DMAD) and 4,5,6,7-tetrahydro-1*H*-pyrrolo[3,2-*c*]pyridines (THPPs), which affords the 4,7,8,9-tetrahydro-1*H*-pyrrolo[2,3-*d*]azocine (THPA) system.[5] In further studies, different activated alkynes have been tested for their ability to promote 6 → 8 ring enlargement on several tetrahydropyridine (THP) substrates, and the results gave ground to attribute this method to the family of general methods. Two years ago, we have reported on a new efficient synthesis of 2,3,6,11-tetrahydro-1*H*-azocino[4,5-*b*]indole and the isomeric 2,3,6,7-tetrahydro-1*H*-azocino[5,4-*b*]indole (THAI) derivatives, starting from hydrogenated β- and γ-carbolines, respectively, and the serendipitous discovery that some of the newly synthesized THAI derivatives inhibit acetylcholinesterase (AChE) in vitro.[6]

AChE inhibition is well recognized as a major pharmacological approach to the treatment of Alzheimer's disease (AD).[7] Current approaches to the treatment of cognitive and behavioral symptoms of AD make use of structurally diverse cholinesterase inhibitors (ChEIs) showing distinct modes of action (Fig. 1). Available ChEI drugs are tacrine (Cognex, **1**),[8] rivastigmine

Keywords: Annulated azocines; Acetylcholinesterase inhibitors; Structure–activity relationships.
* Corresponding author. Tel.: +39 080 5442781; fax: +39 080 5442230; e-mail: altomare@farmchim.uniba.it

0968-0896/$ - see front matter © 2006 Elsevier Ltd. All rights reserved.
doi:10.1016/j.bmc.2006.06.055

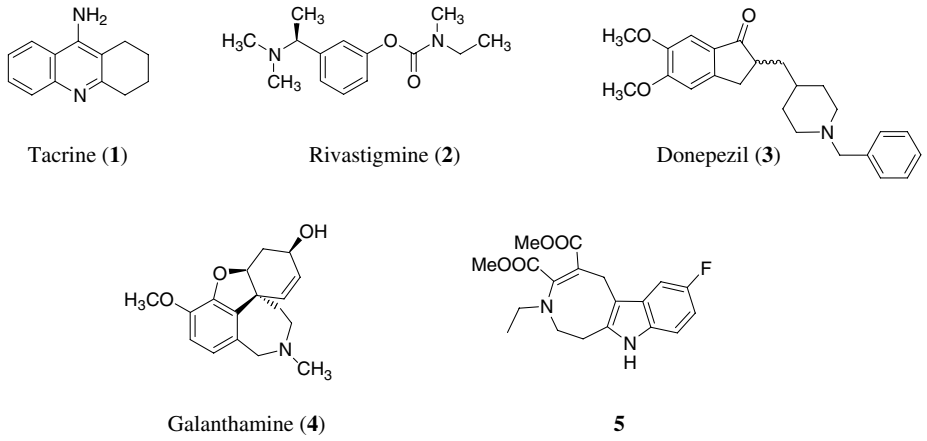

Figure 1. Structures of some known cholinesterase inhibitors.

(Exelon, **2**),[9] donepezil (Aricept, **3**),[10] and galanthamine (Reminyl, **4**).[11] Compounds **1**, **3**, and **4** are reversible inhibitors, whereas **2** acts as a pseudo-irreversible ChEI; they also differ in selectivity toward AChE and butyrylcholinesterase (BuChE).

Two major evidences highlight the central role of AChE in AD: (i) AChE induces the expression of the β-amyloid (Aβ) precursor protein in glia and activates glial cells;[12] (ii) AChE inhibitors, which increase synaptic levels of available acetylcholine (ACh) by preventing its degradation and temporarily slow loss of cognitive function, remain the only approved drugs for the symptomatic treatment of AD.[11] Recent research has revealed that in severe AD brains the levels of AChE are considerably reduced, whereas BuChE activity increases. BuChE may then act as a compensatory mechanism for ACh metabolism,[13] aggravating the toxicity of Aβ.

In a previous study we proved in particular the THA[4,5-*b*]I derivative **5** (Fig. 1) as in vitro AChE inhibitor of moderate potency (IC_{50} = 8.7 μM).[6] With the aim of gaining insights into the structure–activity relationships and possibly identifying new lead/s in AChE inhibitors, in the present work we synthesized some new ester-containing THAI compounds, including [5,4-*b*] ring fusion isomers, and assayed them, as well as a number of other previously synthesized annulated tetrahydroazocines (Chart 1), for their in vitro AChE inhibition. For selected inhibitors we assayed BuChE inhibitory activity, in order to assess the respective ChE selectivity profile, and in vitro monoamine oxidase (MAO) inhibition, which could have neuroprotective benefit in combination with ChE inhibition.[14,15]

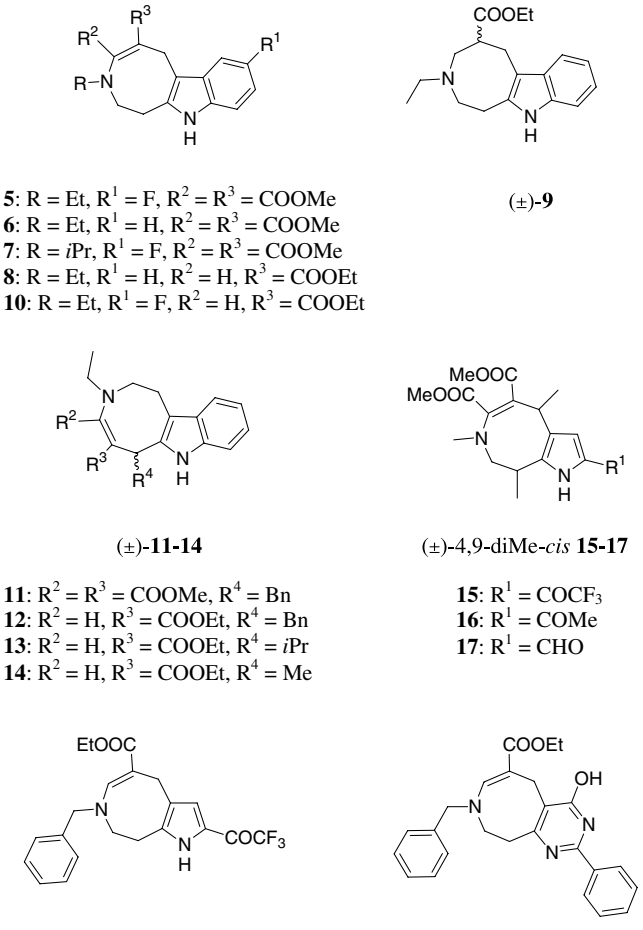

Chart 1.

2. Results and discussion

2.1. Chemistry

Most of the annulated tetrahydroazocines (THA) investigated in this study (Chart 1) have been previously described.[5,6,16,17] The 2,3,6,11-tetrahydro-1*H*-azocino[4,5-*b*]indole (THA[4,5-*b*]I) derivatives (**5**–**8**, **10**) had been synthesized following the procedures developed by some of us.[6] Chemoselective reduction by sodium cyanoborohydride of the enamino derivative **8** afforded the amino compound **9**.

The 2,3,6,7-tetrahydro-1*H*-azocino[5,4-*b*]indole (THA[5,4-*b*]I) derivatives **11** and **12** were synthesized following the synthetic route outlined in Scheme 1. The β-carboline derivative 1-benzyl-2-ethyl-1,2,3,4-tetrahydro-1*H*-pyrido[3,4-*b*]indole, upon treatment with DMAD or ethyl

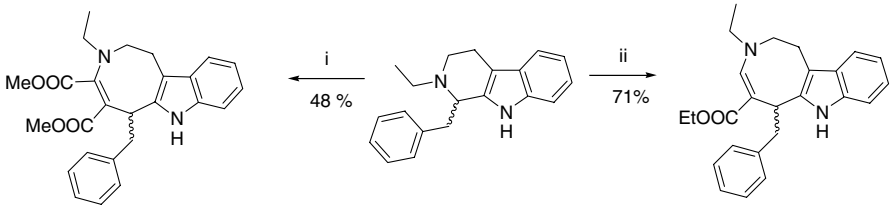

(±)-**11** (±)-**12**

Scheme 1. Reagents and conditions: (i) DMAD/CH_3CN, rt, 24 h; (ii) EP/CH_3CN, rt, 5 h.

propiolate (EP) at room temperature in acetonitrile, provided the target THA[5,4-*b*]I derivatives **11** and **12**, respectively.

Similar to compound **12**, the monoester derivative of 4,7,8,9-tetrahydro-1*H*-pyrrolo[2,3-*d*]azocine (THPA) **18** was synthesized by reacting 2-trifluoroacetyl-5-benzyl-4,5,6,7-tetrahydro-1*H*-pyrrolo[3,2-*c*]pyridine[5a] with EP in dry methanol. A number of already synthesized THPA congeners **15**–**17**,[5,16] bearing 4-CH_3 and 9-CH_3 in *cis*-position, and the 2-phenyl-pyrimidin-4-ol analog **19**[17] have been also included in the molecular dataset in order to extend our investigation of SARs. Chiral compounds **9** and **11**–**17** were synthesized and tested as racemic mixtures, the investigation of enantioselective effects being out of the scope of this work.

2.2. Biological studies

The AChE inhibitory activity of the mono- and diester THA derivatives was assayed by the method of Ellman et al.[18] on AChE from bovine erythrocytes. All compounds were tested in at least five concentrations covering the range producing less than 20% and greater than 80% inhibition, but limited to 100 μM. Concentration-inhibition curves were obtained for most of them and their inhibitory concentration (IC_{50}) calculated by non-linear regression (Table 1). The most active compounds were assayed with the same method for the inhibitory activity of equine serum BuChE in order to assess the ChE selectivity profiles. It is worth noting that bovine AChE and equine BuChE display more than 90% homology with the corresponding human enzymes.[19,20] For comparison, tacrine (**1**) was tested in the same assay conditions, showing mean IC_{50} values of 0.12 and 0.049 μM in the AChE and BuChE inhibition assays, respectively.

The highest AChE inhibitory potency was displayed by compounds **11** and **15**, whose mean IC_{50} values (5.2 μM) are close to that measured by others for galanthamine (GAL) **4** (ca. 3 μM),[21] but one magnitude order lower than the IC_{50} value of tacrine (**1**). More than half test compounds, belonging to THAI, irrespective of the ring

Table 1. Cholinesterase (ChE) and monoamine oxidase (MAO) inhibition activities, and physicochemical parameters of annulated tetrahydroazocine derivatives **5**–**19** (Chart 1)

Compound	ChE inhibition, IC_{50} (μM)[a]		% MAO inhibition[e]		pK_a[f]	log P[f]
	AChE	BuChE	MAO-A	MAO-B		
5	8.7 ± 1.1[b]		5 ± 0.5	n.i.	6.12 ± 0.04	2.23 ± 0.10
6	>100 (32%)					
7	26 ± 1.4				6.71 ± 0.07	2.54 ± 0.05
8	15 ± 1.4				8.89 ± 0.01	2.60 ± 0.04
9	>100 (42%)				8.25 ± 0.03	2.31 ± 0.07
10	8.4 ± 1.1	100 [d]	21 ± 0.8	5 ± 0.7	8.15 ± 0.11	2.79 ± 0.09
11	5.2 ± 1.7	75[d]	5 ± 0.4	n.i.	7.30 ± 0.01	3.15 ± 0.02
12	>20 (22%)[c]		23 ± 0.9	n.i.	8.50 ± 0.19	4.53 ± 0.09
13	42 ± 1.4				9.00 ± 0.15	3.99 ± 0.09
14	37 ± 1.5				8.76 ± 0.12	3.07 ± 0.08
15	5.2 ± 1.5	>100 (34%)	2 ± 0.4	n.i.	5.94 ± 0.01	1.35 ± 0.07
16	>100 (34%)				6.48 ± 0.02	0.90 ± 0.07
17	>100 (31%)					
18	11 ± 2.5		26 ± 0.5	n.i.	6.29 ± 0.03	0.99 ± 0.08
19	22 ± 1.3					

[a] IC_{50}: 50% inhibitory concentration (means ± SEM of three to five experiments) of acetylcholinesterase (AChE, from bovine erythrocytes) or butyrylcholinesterase (BuChE, from equine serum), or % inhibition (average value of three measures in parentheses) at 100 μM concentration.
[b] Value from Ref. 6.
[c] Percent inhibition at the maximum solubility of compound **12**.
[d] Approximated average values, determined by interpolating % inhibitions measured at two inhibitor concentrations.
[e] Percent of MAO-A and -B inhibitory activity as measured at 20 μM concentration; values are means ± SEM of three experiments (n.i. , no inhibition).
[f] Ionization constant (pK_a) and 1-octanol/water partition coefficient (log P) determined by pH-metric technique; values are means ± SD of three to five experiments.

fusion isomerism, and THPA subsets inhibited AChE activity with IC_{50} values in the 10–50 μM range. THA[4,5-*b*]Is **6** and **9**, the low soluble THA[5,4-*b*]I derivative **12**, and THPAs **16** and **17** achieved less than 50% inhibition at the highest concentration tested.

The most active compounds **10**, **11**, and **15**, one for each subset, were chosen for testing in the BuChE assay. They displayed approximate BuChE IC_{50} of 75 μM (**11**) or attained less than 50% inhibition at 100 μM concentration (**15**), whereas compound **10** achieved about 50% inhibition at the highest test concentration (100 μM). All three test compounds proved selective toward AChE with selectivity ratios ranging from about 10 (**10**) to more than 20 (**15**).

Finally, we evaluated the potential MAO inhibition of the azocine derivatives, since this activity could become beneficial in combination with ChE inhibition in treating neurodegenerative diseases.[14,15] The search for new compounds endowed with MAO and dual AChE/MAO inhibition activity constitutes a major purpose of our general research.[22] We measured the MAO inhibitory activity of the most potent AChE inhibitors, two for each subset, at 20 μM concentration. Most of the test compounds exhibited negligible (**5**, **11**, and **15**) or weak activity (**10**, **12**, and **18**), mostly toward MAO-A isoform. A common trait is that within each subset the monoester derivatives showed MAO-A percent inhibition higher compared to the diester congeners.

2.3. Modeling and structure–activity relationship studies

In order to gain insight into binding modes of the most active derivatives **11** and **15** into the active site of AChE, preliminary docking calculations were performed by the QXP software,[23] and the results compared with 3D coordinates of (−)-galanthamine (GAL) **4**, a low-micromolar inhibitor complexed with *Torpedo californica* AChE (*Tc*AChE).[24] The ligand-free *Tc*AChE (PDB entry: 1DX6) was used as the ligate, whereas as starting geometries of the ligands we used a 3D model of **11** (*R* configuration), built up on the crystal structure of compound **13**[6] using fragments from the SYBYL (Ver. 7.1) standard library (Tripos Assoc., St. Louis, MO, USA), and the X-ray 3D structure of **15** (4*R*,9*R* configuration).[5a] Docking calculations were carried out using the MCDOCK module of QXP.[25]

As shown in Figure 2, the diester THA[5,4-*b*]I derivative **11** and the THPA derivative **15** could bind at the base of the active site gorge of *Tc*AChE, interacting with the choline-binding site (Trp84) and the acyl-binding pocket. In both cases, docking models suggest that the double bond α to the azocine tertiary amine group could stack against the Trp84 indole ring, whereas the carbonyl oxygen of the COOMe groups, β and α to azocine nitrogen in **11** and **15**, respectively, could form hydrogen bond (HB) with Ser122. Furthermore, the binding affinity of compound **11** may enhance due to aromatic interactions of the 6-benzyl group with aromatic residues close to the acyl-binding pocket (in particular, π-stacking with Tyr334). The carbonyl oxygen of the 2-$COCF_3$ group in the THPA derivative **15** could form a strong HB with Ser200 and two additional HBs with the backbone NHs of Gly118 and Gly119.

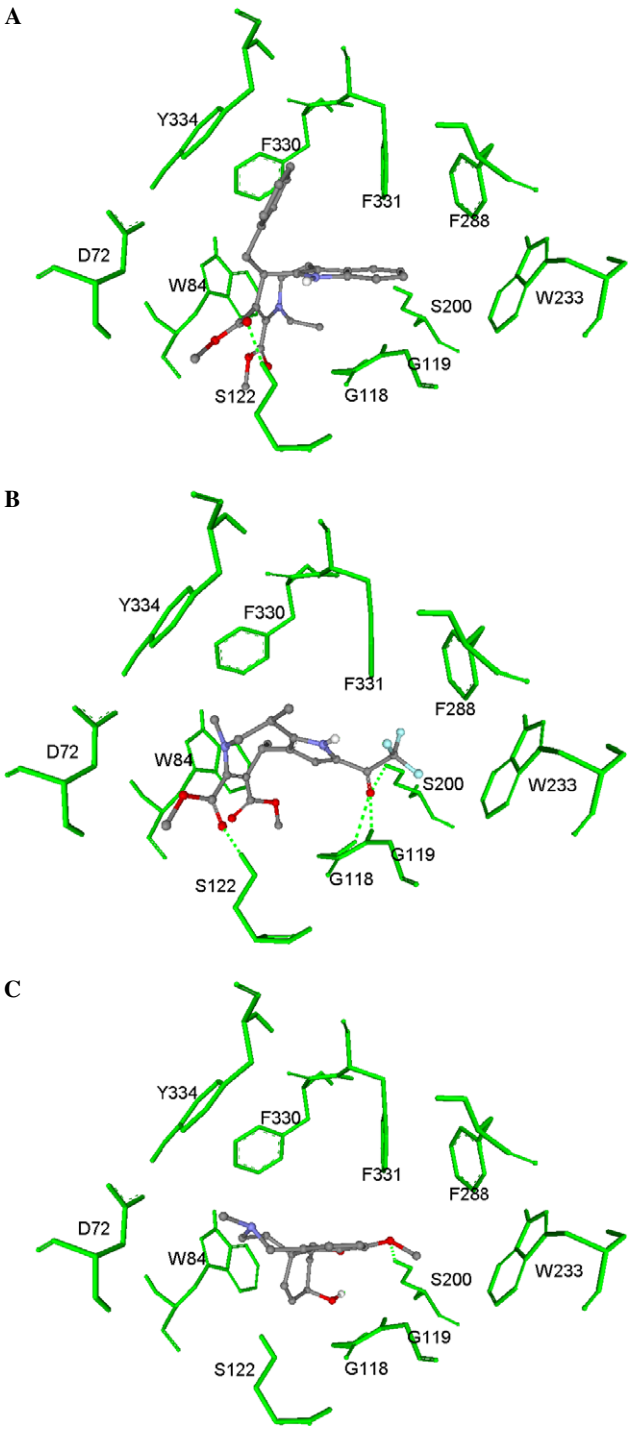

Figure 2. Representations of compounds **11** (A), in *R* configuration, and **15** (B), in 4*R*,9*R* configuration, docked into the binding site of *Tc*AChE, compared with the crystallographic structure of the complex (C) between (−)-GAL **4** and *Tc*AChE (PDB entry: 1DX6). The inhibitors are displayed as ball-and-stick models colored by atom type. The protein residues in a distance of 5 Å from the inhibitor are rendered as green-colored stick models with hydrogen bonds in evidence.

In connection with the AChE inhibitory activity, within each subset the test compounds span about the same range of IC_{50} values, suggesting that the AChE inhibition activity does not strictly depend either on the fused N-heterocycle (i.e., pyrrole or indole) or on ring fusion isomerism (i.e., [4,5-*b*] or [5,4-*b*]) for the indole-containing derivatives. Even though the most potent inhibitors **11** and **15** are both diesters, the presence of two COOMe groups does not appear as a requisite for enhancing AChE inhibitory activity. Notable inhibition potencies were indeed shown by compounds bearing only one COOEt group β to azocine nitrogen, which are equipotent to (**10**), more potent (**8**) or less potent (**12**) than the corresponding diester derivatives (**5**, **6**, and **11**, respectively).

Examining AChE inhibition data suggested the following qualitative SARs: (i) the introduction of a fluorine atom at position 8 in THA[4,5-*b*]I subset (R^1 on the indole substructure) results in enhancing inhibition potency (compare **5** with **6**, and **8** with **10**); (ii) even slightly increasing steric hindrance of the alkyl group on the azocine nitrogen results in decreasing the inhibitory potency, as proven by the about threefold increase of IC_{50} value (compare the *N*3-ethyl derivative **5** with the *N*3-isopropyl derivative **7**); (iii) reduction of the 4,5-double bond, which should in principle enhance basicity of the amino group and decrease lipophilicity, results in decreased potency (compare compounds **8** and **9**); (iv) lipophilicity of the R^4 alkyl groups in THA[5,4-*b*]I subset and the R^1 substituents at position 2 of the THPA scaffold seems to play a role. Indeed, activity increases with decreasing lipophilicity of the R^4 alkyl groups in THA[5,4-*b*]I derivatives **12**–**14** and with increasing lipophilicity of the R^1 substituents in THPA derivatives **15**–**17**, suggesting a parabolic or bilinear relationship between AChE inhibition data and lipophilicity, with the less lipophilic THPA derivatives on the ascending side and more lipophilic THA[5,4-*b*]I derivatives on the descending side of the curve.

With the aim of investigating such a possible relation, we measured 1-octanol/water partition coefficients (log *P*) of the compounds having finite AChE IC_{50} values, using a reliable pH-metric technique.[26] Due to the low solubility in water, the aqueous pK_a values of the THA derivatives were assessed from at least three measurements carried out in water/methanol mixtures through Yasuda–Shedlovsky extrapolation.[27] log *P* values were obtained, after additional titrations in 1-octanol/water mixtures (Table 1).

In the examined series, the variation of the ionization constants depends mainly upon the presence of the methyl (or ethyl) carboxylate groups, the monoester derivatives spanning the pK_a range 8.15–9.00 and the diester derivatives spanning the pK_a range 5.94–7.30, meaning that the fraction of protonated THA at pH 8.0 should vary as between ca. 1% and 15% for the diester derivatives and between ca. 60% and 90% for the monoester derivatives.

To retain SAR information, AChE pIC_{50}s of compounds **12** and **16** were estimated by extrapolation at

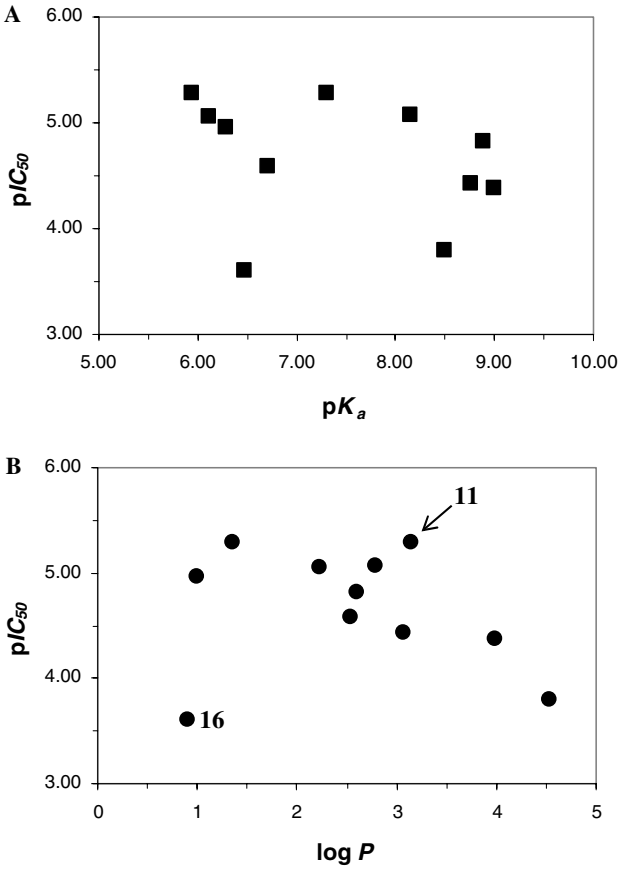

Figure 3. Scatter plots of AChE pIC_{50} versus (A) pK_a and (B) log *P* of the tetrahydroazocine derivatives. In plot (B), when omitting compound **16**, the data fit a parabolic relationship with $r^2 = 0.665$.

3.80 and 3.60, respectively, and included in the dataset. Inspection of the plots of pIC_{50} against pK_a (Fig. 3A) did not reveal any relation of significance, suggesting that the AChE inhibition potency of the THA derivatives is not significantly affected by the degree of protonation of the azocine amino group. In contrast, the plot of pIC_{50} against log *P* (Fig. 3B), even showing a certain spread of the data, suggested a trend. A reasonable parabolic correlation was indeed obtained between pIC_{50} and log *P* ($r^2 = 0.665$), when omitting compound **16** as the strongest outlier with respect to the prevailing behavior. These results pointed out that, albeit insufficient alone for effective activity prediction, log *P* is somehow related to the inhibition potency of the annulated THA derivatives studied.

The most active derivative **11** showed an inhibition potency higher than that expected from the parabolic relationship, most likely due to the additional (not accounted for by the log *P* parameter) aromatic interactions of the 6-benzyl group, as highlighted by docking results.

3. Conclusions

A number of ester derivatives of annulated 1,2,3,6-tetrahydroazocines described herein, which can be efficiently

synthesized through 6 → 8 ring expansion of THP-containing substrates under the action of DMAD or EP, exhibited AChE inhibition in vitro. Dimethyl 3-ethyl-6-benzyl-2,3,6,7-tetrahydro-1*H*-azocino[5,4-*b*]indole-4,5-dicarboxylate (**11**) and dimethyl 4,7,9-trimethyl-2-(trifluoroacetyl)-4,7,8,9-tetrahydro-1*H*-pyrrolo[2,3-*d*]azocine-5,6-dicarboxylate (**15**) proved the most potent ones, both with IC_{50} value in the low-micromolar range, and quite selective in inhibiting AChE as compared with BuChE. None of the investigated compounds showed appreciable in vitro MAO inhibitory activity.

A preliminary molecular modeling study based on docking calculations between these compounds and the 3D X-ray structure of *Tc*AChE provided support to the hypothesis that compounds **11** and **15** can bind at the base of the active site gorge, interacting with choline-binding site (Trp84), aromatic residues (compound **11**) close to the acyl-binding pocket and, through HBs, with key Ser residues (Ser200 and Ser122). Moreover, a likely parabolic relationship between pIC_{50} and log*P* (and not the degree of protonation of azocine nitrogen), describing the prevailing behavior of the studied annulated THA derivatives, suggests that lipophilicity plays a role in modulating the AChE inhibitory potency.

4. Experimental

4.1. Chemistry

All solvents were distilled and dried before use, DMAD and EP were purchased from Lancaster Synthesis Ltd. and were used without any additional purification. Column chromatography was performed with alumina oxide 60 from Fluka. ^1H and ^{13}C NMR spectra were recorded in $CDCl_3$ solutions, at 25 °C or in DMSO-d_6 solutions at 40 °C, using a Bruker WM 400 NMR spectrometer operating at 400 and 100 MHz correspondingly, peak positions are given in parts per million (δ) with tetramethylsilane used as the internal standard. The following abbreviations were used: s, singlet; d, doublet; t, triplet; q, quartet; dd, double doublet; m, multiplet; br, broad. Mass spectra were obtained by ESI method (Agilent 1100 Series LC/MSD Trap System VL). Melting points were determined in a capillary tube and are uncorrected. Compounds **5**–**8**, **10**, **13** and **14**,[6] **15**,[5a] **16**,[16] **17**,[5a] and **19**[17] were synthesized according to previously reported protocols.

4.2. Ethyl 3-ethyl-2,3,4,5,6,11-hexahydro-1*H*-azocino[4,5-*b*]-indole-5-carboxylate (9)

To a vigorously stirred solution of 150 mg (0.5 mmol) of tetrahydroazocine **8** in 10 mL of methanol, containing 0.2 mL of glacial acetic acid, 32 mg (0.5 mmol) of $NaCNBH_3$ was added in three portions. The reaction mixture was refluxed for 2 h (TLC monitoring). After the completion of the reaction, methanol was evaporated, the residue was worked up with 10 mL of water and extracted with EtOAc (3× 50 mL). The organic extract was dried over $MgSO_4$ and evaporated to dryness. The oily residue (140 mg) was percolated through a short column with Al_2O_3 (EtOAc/hexane 1:3), yielding 120 mg (80%) of **9** as a pale-yellow viscous oil. ^1H NMR ($CDCl_3$) δ 1.02 (t, 3H, J = 7.2 Hz, CH_3CH$_2$N), 1.26 (t, 3H, J = 7.1 Hz, CH_3CH$_2$O), 2.52 (dd, 1H, J = 14.3, 4.3 Hz, H-4), 2.65–2.92 (m, 8H), 3.19 (dd, 1 H, J = 14.2, 5.2 Hz, H-6), 3.31 (dd, 1H, J = 14.2, 8.3 Hz, H-6), 4.15 (q, 2H, J = 7.1 Hz, CH$_3$CH_2O), 7.00–7.12 (m, 2H, H-8, H-9), 7.27 (dd, 1H, J = 7.9, 1.2 Hz, H-7), 7.55 (dd, 1H, J = 7.9, 1.2 Hz, H-10), 7.84 (br, 1H, NH). ^{13}C NMR ($CDCl_3$) δ 12.3, 15.1, 22.0, 23.8, 43.7, 50.0, 52.3, 56.5, 61.2, 108.3, 110.2, 117.6, 119.7, 124.2, 130.1, 135.2, 137.8, 165.7. ESI MS 301 (M^++1). Anal. Calcd for $C_{18}H_{24}N_2O_2$: C, 71.97; H, 8.05; N, 9.33. Found: C, 71.25; H, 8.58; N, 9.52.

4.3. General procedure for the preparation of derivatives 11 and 12

To a stirred solution of 1-benzyl-2-ethyl-1,2,3,4-tetrahydro-1*H*-pyrido[3,4-*b*]indole (290 mg, 1 mmol) in 10 mL of acetonitrile 1.2 mmol of DMAD or EP was added in one portion. Stirring was continued for additional 24 h (in the case of DMAD) or 5 h (in the case of EP). After the completion of the reaction (TLC monitoring) solvent was evaporated under reduced pressure. The residue was purified by column chromatography (in the case of DMAD) or by re-crystallization from ethyl acetate (in the case of EP).

4.3.1. Dimethyl 3-ethyl-6-benzyl-2,3,6,7-tetrahydro-1*H*-azocino[5,4-*b*]indole-4,5-dicarboxylate (11). 48%, yellow crystals with mp 148–150 °C (ethyl acetate/hexane). ^1H NMR ($CDCl_3$) δ 1.12 (t, 3H, J = 7.0 Hz, CH_3CH$_2$), 2.74 (m, 2H, CH$_2$-1), 3.01–3.21 (m, 2H, CH$_2$–Ph), 3.25 (q, 2H, J = 7.0 Hz, CH_2CH$_3$), 3.65 (m, 2H, CH$_2$-2), 3.70 (s, 3H, OMe), 3.78 (s, 3H, OMe), 4.53 (dd, 1H, J = 10.1, 4.0 Hz, H-6), 6.93–7.82 (m, 9H, Ar), 8.01 (br, 1H, NH). ^{13}C NMR ($CDCl_3$) δ 12.1, 27.2, 34.9, 35.1, 47.1, 55.2 (2 × C), 58.0, 108.2, 110.6, 114.5, 116.4, 119.2, 123.0, 125.1, 128.3 (2 × C), 128.5 (2 × C), 128.9, 131.2, 135.7, 138.8, 139.2, 165.1, 166.0. ESI MS 433 (M^++1). Anal. Calcd for $C_{26}H_{28}N_2O_4$: C, 72.20; H, 6.53; N, 6.48. Found: C, 69.32; H, 6.12; N, 6.14.

4.3.2. Ethyl 3-ethyl-6-benzyl-2,3,6,7-tetrahydro-1*H*-azocino[5,4-*b*]indole-5-carboxylate (12). 71%, pale-yellow crystals with mp 246–248 °C (ethyl acetate/hexane). ^1H NMR ($CDCl_3$) δ 1.20 (t, 3H, J = 7.0 Hz, CH_3CH$_2$N), 1.28 (t, 3H, J=7.1 Hz, CH_3CH$_2$O), 3.11–3.27 (m, 4H, CH$_2$-1, CH$_2$–Ph), 3.30–3.37 (m, 2H, CH$_3$CH_2N), 3.65 (dd, 1H, J = 14.0, 4.0 Hz, CH-2), 4.15 (q, 2H, J = 7.1 Hz, CH$_3$CH_2O), 4.21 (dd, 1H, J = 14.0, 10.2 Hz, CH-2), 4.64 (dd, 1H, J = 10.2, 4.0 Hz, CH-6), 7.04–7.15 (m, 4H, Ar), 7.26 (s, 1H, 4-H), 7.45–7.47 (m, 5H, Ar), 7.67 (br, 1H, NH). ^{13}C NMR ($CDCl_3$) δ 12.5, 15.2, 28.3, 29.4, 35.2, 51.3, 58.2, 60.0, 101.2, 107.3, 114.1, 118.2, 119.5, 125.0 (2 × C), 128.1, 130.0, 131.2 (2 × C), 132.0, 133.1, 136.2, 137.1, 145.1, 162.2. ESI MS 389 (M^++1). Anal. Calcd for $C_{25}H_{28}N_2O_2$: C, 77.29; H, 7.26; N, 7.21. Found: C, 77.21; H, 7.41; N, 7.42.

4.4. Ethyl 7-benzyl-2-(2,2,2-trifluoroacetyl)-4,7,8,9-tetrahydro-1*H*-pyrrolo[2,3- *d*]azocine-5-carboxylate (18)

Eighty milligrams (0.75 mmol) of EP was added in one portion to the solution of 230 mg (0.75 mmol) of 2-trifluoroacetyl-5-benzyl-4,5,6,7-tetrahydro-1*H*-pyrrolo[3,2-*c*]pyridine[5a] in 5 mL of dry methanol and the reaction mixture was stirred at room temperature for 72 h (TLC monitoring). The solvent was evaporated under reduced pressure and the residue was recrystallized from ethyl acetate/hexane mixture, providing 240 mg (78%) of **18** as white crystals with mp 164–165 °C. ^{1}H NMR ($CDCl_3$) δ 1.29 (t, 3H, $J = 7.3$ Hz, CH_3CH_2), 2.87 (t, 2H, $J = 5.8$ Hz, CH_2-9), 3.81 (s, 2H, 4-CH_2), 3.90 (t, 2H, $J = 5.8$ Hz, CH_2-8), 4.18 (q, 2H, $J = 7.3$ Hz, OCH_2), 4.35 (s, 2H, CH_2–Ph), 6.99 (m, 1H, H-3), 7.20–7.35 (m, 5H, Ph), 7.56 (s, 1H, H-6), 9.04 (br, 1H, NH). ESI MS 407 (M^++1). Anal. Calcd for $C_{21}H_{21}F_3N_2O_3$: C, 61.21; H, 4.85; N, 7.14. Found: C, 61.25; H, 4.58; N, 6.88.

4.5. Determination of pK_a and log *P* by the pH-metric technique

The Sirius GLpKa (Sirius Analytical Instruments Ltd., Forest Row, East Sussex, UK) computerized titration instrument was used to determine pK_a and log *P* values in *n*-octanol/water biphasic system at 25 ± 0.5 °C of a number of fused azocine derivatives. All experiments were carried out in triplicate under a slow argon flow. Details about instrument and procedures can be found elsewhere.[26]

To determine pK_a value, a right amount of each compounds was dissolved in 20 mL of ionic strength adjusted water (0.15 M KCl), to achieve final sample concentration of about 5×10^{-4} M. All titrations were recorded in the pH range between 1.8 and 12 at 25 ± 0.5 °C, using standardized 0.5 M HCl and 0.5 M carbonate-free KOH as titrating agents. The maximum titrant volume increment for one titration step was limited to 0.25 mL. The pH change per titrant addition was limited to 0.2 pH units and pH value in each point was collected when the pH-drift was lower than 0.002 pH per minute. Bjerrum plots[26] were used to calculate precise pK_a values. For compounds with low aqueous solubility, methanol ranging from 8% to 45% v/v was added as the cosolvent, and aqueous pK_a values were obtained by extrapolation using the Yasuda–Shedlovsky procedure.[27]

The log *P* values were determined by potentiometric titrations carried out in the biphasic system constituted by 0.15 M KCl aqueous solution and water-saturated 1-octanol. Titration curves were recorded in the presence of different volumes of 1-octanol (at least three different 1-octanol/water v/v ratios depending upon the compound lipophilicity) and the results plotted against logarithm of phase ratio.[28] All data were processed by using RefinementPro software (Sirius Analytical Instruments Ltd., Forest Row, East Sussex, UK).

4.6. Cholinesterase inhibition assay

Compounds were evaluated using AChE from bovine erythrocytes and BuChE from equine serum (Sigma) following the method of Ellman et al.[18] The AChE activity was determined in a reaction mixture containing 200 μL of a solution of AChE (0.415 U/mL in 0.1 M phosphate buffer, pH 8.0), 100 μL of a solution of 5,5′-dithio-bis(2-nitrobenzoic) acid (DTNB 3.3 mM in 0.1 M phosphate-buffered solution, pH 7.0, containing $NaHCO_3$ 6 mM), 100 μL of a solution of the inhibitor (five to seven concentrations, ranging from 1×10^{-7} to 1×10^{-4} M), and 500 μL of phosphate buffer, pH 8.0. After incubation for 20 min at 25 °C, acetylthiocholine iodide (100 μL of 0.05 mM water solution) was added as the substrate, and AChE activity was determined by UV spectrophotometry from the absorbance changes at 412 nm for 3.0 min at 25 °C. The concentration of compound which produced 50% inhibition of the AChE activity (IC_{50}) was calculated by nonlinear regression of the response–concentration (log) curve. BuChE inhibitory activity determinations were carried out similarly using butyrylthiocholine iodide (0.05 mM) as the substrate. Results are reported as means ± SEM of IC_{50} obtained from at least three independent measures.

4.7. Monoamine oxidase inhibition assay

MAO inhibitory activity of selected compounds (**5**, **10**–**12**, **15**, and **18**) at 20 μM concentration was determined using a continuous spectrophotometric assay,[29] monitoring the rate of oxidation of the nonselective MAO substrate kynuramine to 4-hydroxyquinoline. Briefly, male Sprague–Dawley rats (200–250 g) were sacrificed by decapitation. The brains were immediately removed and washed in an ice-cold isotonic Na_2HPO_4/KH_2PO_4 buffer (pH 7.4) containing sucrose. A crude brain mitochondrial fraction was then prepared by differential centrifugation and stored at −40 °C in an isotonic Na_2HPO_4/KH_2PO_4 buffer (pH 7.4) containing KCl. MAO-A and MAO-B activities in mitochondrial preparations (1 mg/mL) were assayed using as selective and irreversible inhibitors (−)L-deprenyl (250 nM) and clorgyline (250 nM), respectively.[30] After a pre-incubation for 5 min with the assayed compound dissolved in DMSO at a final concentration of 5% (v/v), kynuramine was added at a concentration equal to the corresponding K_M value (90 μM for MAO-A and 60 μM for MAO-B), and the rate of formation of 4-hydroxyquinoline was monitored at 314 nm for 5 min.

Acknowledgments

The Italian authors thank the Italian Ministry for Education, Universities and Research (MIUR, Rome, PRIN 2004, Grant No. 2004037521 006) for financial support. The Russian authors thank the Russian foundation for basic research (Grant No. 05-03-08149-OFI-A) for supporting this work. The Spanish authors thank the Ministry of Education and Science, and the European Regional Development Fund (Madrid, Spain, Grant BFI2003-00493) for financial support.

References and notes

1. Bertha, C. M.; Ellis, M.; Filippen-Anderson, J. L.; Porreca, F.; Rothman, R. B.; Davis, P.; Xu, H.; Becketts, K.; Rice, K. C. *J. Med. Chem.* **1996**, *38*, 2081.
2. Alvarez, M.; Joule, A. *Alkaloids*; Chemistry and Biology; Academic Press: New York, 2001; Vol. 57, pp 235–272.
3. (a) Bennasar, M.-L.; Zulaica, E.; Ramirez, A.; Bosch, J. *Tetrahedron* **1999**, *55*, 3117; (b) Alazard, J.-P.; Millet-Paillusson, C.; Guenard, D.; Thal, C. *Bull. Soc. Chim. Fr.* **1996**, *133*, 251.
4. Gil, L.; Gil, R. P. d. F.; dos Santos, D. C.; Marazano, C. *Tetrahedron Lett.* **2000**, *41*, 6067.
5. (a) Varlamov, A. V.; Borisova, T. N.; Voskressensky, L. G.; Kulikova, L. N.; Soklakova, T. A.; Chernyshev, A. I.; Alexandrov, G. G. *Tetrahedron Lett.* **2002**, *43*, 6767; (b) Varlamov, A. V.; Borisova, T. N.; Voskressensky, L. G. *Synthesis* **2002**, *2*, 155.
6. Voskressensky, L. G.; Borisova, T. N.; Kulikova, L. N.; Varlamov, A. V.; Catto, M.; Altomare, C.; Carotti, A. *Eur. J. Org. Chem.* **2004**, 3128.
7. (a) Carreiras, M. C.; Marco, J. L. *Curr. Pharm. Des.* **2004**, *10*, 3167; (b) O'Neill, M. F. *Drug Discovery Today* **2005**, *10*, 1333.
8. Davis, K. L.; Powchik, P. *Lancet* **1995**, *345*, 625.
9. Prous, J.; Rabasseda, X.; Castaner, J. *Drugs Future* **1996**, *19*, 656.
10. Sugimoto, H.; Iimura, Y.; Yamanishi, Y.; Yamatsu, K. *J. Med. Chem.* **1995**, *38*, 4821.
11. Michaelis, M. L. *J. Pharmacol. Exp. Ther.* **2003**, *304*, 897.
12. Grossberg, G. T. *Int. Psychogeriatr.* **2002**, *14*(Suppl. 1), 27.
13. Darvesh, S.; Hopkins, D. A.; Geula, C. *Nat. Rev. Neurosci.* **2003**, *4*, 131.
14. Fawcett, J. R.; Bordayo, E. Z.; Jackson, K.; Liu, H.; Peterson, J.; Svitak, A.; Frey, W. H., 2nd *Brain Res.* **2002**, *950*, 10.
15. Weinstock, M.; Poltyrev, T.; Bejar, C.; Youdim, M. H. *Psychopharmacology* **2002**, *160*, 318.
16. Voskressensky, L. G.; Borisova, T. N.; Soklakova, T. A.; Kulikova, L. N.; Borisov, R. S.; Varlamov, A. V. *Lett. Org. Chem.* **2005**, *2*, 18.
17. Voskressensky, L. G.; Borisova, T. N.; Kostenev, I. S.; Kulikova, L. N.; Varlamov, A. V. *Tetrahedron Lett.* **2006**, *47*, 999.
18. Ellman, G. L.; Courtney, K. D.; Andres, V., Jr.; Feather-Stone, R. M. *Biochem. Pharmacol.* **1961**, *7*, 88.
19. Cygler, M.; Schrag, J. D.; Sussman, J. L.; Harel, M.; Silman, I.; Gentry, M. K.; Doctor, B. P. *Protein Sci.* **1993**, *2*, 366.
20. Kovarik, Z.; Bosak, A.; Sinko, G.; Latas, T. *Croat. Chem. Acta* **2003**, *76*, 63.
21. Barreiro, E. J.; Camara, C. A.; Verli, H.; Brazil-Más, L.; Castro, N. G.; Cintra, W. M.; Aracava, Y.; Rodrigues, C. R.; Fraga, C. A. M. *J. Med. Chem.* **2003**, *46*, 1144.
22. (a) Gnerre, C.; Catto, M.; Leonetti, F.; Weber, P.; Carrupt, P.-A.; Altomare, C.; Carotti, A.; Testa, B. *J. Med. Chem.* **2000**, *43*, 4747; (b) Bruhlmann, C.; Ooms, F.; Carrupt, P.-A.; Testa, B.; Catto, M.; Leonetti, F.; Altomare, C.; Carotti, A. *J. Med. Chem.* **2001**, *44*, 3195; (c) Carotti, A.; Altomare, C.; Catto, M.; Gnerre, C.; Summo, L.; De Marco, A.; Rose, S.; Jenner, P.; Testa, B. *Chem. Biodiv.* **2006**, *3*, 134.
23. McMartin, C.; Bohacek, R. S. *J. Comput. Aided Mol. Des.* **1997**, *11*, 333.
24. Greenblatt, H. M.; Kryger, G.; Lewis, T.; Silman, I.; Sussman, J. L. *FEBS Lett.* **1999**, *463*, 321.
25. In order to generate suitable docking poses of the ligand structures **11** and **15**, with a good sampling of the conformational space, 500 runs of Monte Carlo search followed by conjugate gradient minimization were performed, resulting in 20 low-energy docking solutions. The lowest-energy docked structures (i.e., complexes within 1 kcal/mol range from the minimum-energy MCDOCK solution) were compared to the X-ray structure of galanthamine.
26. (a) Avdeef, A. *Quant. Struct.-Act. Relat.* **1992**, *11*, 510; (b) Avdeef, A. *J. Pharm. Sci.* **1993**, *82*, 183; (c) Avdeef, A.; Box, K. J.; Comer, J. E. A.; Hibbert, C.; Tam, K. Y. *Pharm. Res.* **1998**, *15*, 209.
27. Takács-Novák, K.; Box, K. J.; Avdeev, A. *Int. J. Pharm.* **1997**, *151*, 235.
28. Kraemer, S. D.; Gautier, J.-C.; Saudemon, P. *Pharm. Res.* **1998**, *15*, 1310.
29. Méndez-Álvarez, E.; Soto-Otero, R.; Sánchez-Sellero, I.; López-Rivadulla Lamas, M. *Life Sci.* **1997**, *60*, 1719.
30. Soto-Otero, R.; Méndez-Álvarez, E.; Hermida-Ameijeiras, A.; Sánchez-Sellero, I.; Cruz-Landeira, A.; López-Rivadulla Lamas, M. *Life Sci.* **2001**, *69*, 879.